Primary Structure of and Studies on *Acanthamoeba* Actophorin†

Stephen Quirk,‡,§ Sutherland K. Maciver,§,∥ Christophe Ampe,⊥ Stephen K. Doberstein,§ Donald A. Kaiser,§ Jozef VanDamme,⊥ Joel S. Vandekerckhove,⊥ and Thomas D. Pollard*,§

Department of Biophysics and Biophysical Chemistry and Department of Cell Biology and Anatomy, The Johns Hopkins Medical School, Baltimore, Maryland 21205, and Laboratory of Physiological Chemistry, The University of Ghent, Ghent, Belgium

Received March 23, 1993; Revised Manuscript Received June 7, 1993

ABSTRACT: We determined the amino acid sequence of the actin monomer binding/actin filament severing protein actophorin from *Acanthamoeba castellanii* by automated Edman degradation of peptide fragments and by sequencing of full-length cDNA. Actophorin consists of 138 amino acids (calculated molecular weight of 15 543) and shares a high degree of sequence similarity to other low molecular weight actin monomer sequestering proteins, especially vertebrate cofilin, vertebrate actin depolymerizing factor/destrin, and echinoderm depactin. Actophorin is smaller and does not contain a nuclear localization sequence like the related vertebrate proteins. Southern blot analysis indicates that actophorin is a single-copy gene; however, Northern blots show two distinct mRNA species of 1 and 0.9 kb in size. Homogeneous recombinant actophorin purified from *Escherichia coli* is indistinguishable from the native protein in its physical properties and in biochemical assays of its interaction with actin, but is less reactive with three monoclonal antibodies raised against the native protein. The NH_2 terminus of native actophorin is blocked, while the initiating methionine residue is removed from recombinant actophorin. This difference has no measurable effect on activity. By fluorescent antibody staining of *Acanthamoeba*, actophorin colocalizes with actin filaments in the cortical cytoplasm, especially at the leading edge of the cell. Additionally, actophorin binds phosphatidylinositol 4′,5′-bisphosphate. The recombinant actophorin forms X-ray diffraction quality crystals of superior quality in poly(ethylene glycol)/2-propanol and, like the native crystal form, belongs to space group $P2_12_12_1$.

Acanthamoeba actophorin is a low molecular weight actin monomer binding/actin filament severing protein (Cooper et al., 1986; Maciver et al., 1991) that shares some functional properties with two vertebrate proteins, actin depolymerizing factor, ADF (Bamburg et al., 1980; Adams et al., 1990; Abe et al., 1990), and destrin (Nishida et al., 1985; Moriyama et al., 1990b), and with echinoderm egg depactin (Mabuchi, 1981; Takagi et al., 1988). The vertebrate proteins are homologues of each other and of depactin. Surprisingly, all of these proteins are similar in sequence to cofilin (Nishida et al., 1984; Yonezawa et al., 1985; Abe et al., 1990; Matsuzaki et al., 1990; Adams et al., 1990; Moriyama et al., 1990a), another vertebrate actin binding protein with distinct properties including time and place of expression (Abe et al., 1990; Ohta et al., 1989) and high affinity for actin filaments (Yonezawa et al., 1985; Nishida, 1985). Polyphosphoinositides inhibit the binding of cofilin and destrin to actin (Yonezawa et al., 1990). These proteins may regulate actin polymerization in the cell by severing actin filaments and/or by sequestering actin monomers, but their physiological functions are far from clear.

Actophorin isolated from *Acanthamoeba castellanii* is a 15-kDa protein with two established biochemical activities. First, by forming a 1:1 complex with monomeric actin (Cooper et al, 1986; Maciver et al., 1991), actophorin can regulate the pool of actin available for polymerization. Second, actophorin severs actin filaments in a dose-dependent manner. Both sequestering and severing are inhibited by orthophosphate (Maciver et al., 1991). In the presence of the cross-linking protein α-actinin, actin filament severing by actophorin promotes the formation of rigid actin bundles that are visible by light microscopy (Maciver et al., 1991b).

In this paper, we present the primary structure of actophorin, characterize recombinant actophorin isolated in high yield from *Escherichia coli*, and localize the protein in the cortex of *Acanthamoeba* with fluorescent antibodies. The sequence of actophorin is closer to that of cofilin than to the ADF group with which it shares more functional properties. Although recombinant actophorin lacks the modified NH_2-terminal methionine, it is indistinguishable from the native protein in its physical and functional properties except for reduced reactivity with three monoclonal antibodies.

MATERIALS AND METHODS

General Molecular and Biochemical Procedures. Unless otherwise noted, all procedures performed in this study are according to Maniatis et al. (1982) or Sambrook et al. (1989), including bacteria and phage plating, agarose gel electrophoresis, restriction endonuclease digestions, library screening, and Southern and Northern blotting. Chemical reagents were from Sigma Chemical Co. (St. Louis, MO) unless specifically mentioned. Protein concentration was determined either by using the method of Bradford (1976) with bovine serum albumin as standard or by monitoring the absorbance at 280 nm (a 1 mg/mL solution of actophorin has an A_{280} value of 0.89; Cooper et al., 1986).

† This research was supported by NIH Research Grants GM-26338 and GM-35171. An NSF Biological Centers Award, (DIR-8721059) and the W. M. Keck Foundation in part supported this study. An Institute for Biophysical Research on Macromolecular Assemblies postdoctoral fellowship was awarded to S.Q. and S.K.M. was supported by a postdoctoral fellowship from the Muscular Dystrophy Association.

* Correspondence should be addressed to this author. Telephone: (410) 955-5664. FAX: (410) 955-4129.

‡ Department of Biophysics and Biophysical Chemistry, The Johns Hopkins Medical School.

§ Department of Cell Biology and Anatomy, The Johns Hopkins Medical School.

∥ Present address: MRC Laboratory of Molecular Biology, Cambridge, England.

⊥ The University of Ghent.

0006-2960/93/0432-8525$04.00/0

Native Protein Purification and Peptide Sequencing. Native actophorin was purified from *Acanthamoeba castellanii* according to Cooper et al. (1986). Peptides were generated from actophorin by the method of Ampe et al. (1988). Briefly, 200 μg of actophorin was cleaved with either trypsin, cyanogen bromide (CNBr), or 2-[(2-nitrophenyl)-sulfenyl]-3-methyl-3-bromoindolenine (BNPS-skatole). The resulting peptides were separated by HPLC on a C4 reversed-phase column (0.46 × 25 cm; Vydac Separations Group, Hesperia, CA). Peptides were eluted at 1 mL/min with a linear gradient of 0–70% acetonitrile in 0.1% trifluoroacetic acid. The gradient was started 5 min after sample loading. Peptides were detected by the absorbance at 214 nm, collected manually in 1.5-mL Eppendorf tubes, and dried in a Rotovac prior to storage at −20 °C. Edman degradation was carried out on an Applied Biosystems Inc 470 A gas-phase sequenator, and the amino acids were determined with a 120 A phenylthiophydantoin amino acid analyzer following manufacturer instructions.

Isolation of an Actophorin cDNA Clone. An *Acanthamoeba* λgt10 cDNA library (Pollard & Rimm, 1991) was screened with two oligonucleotides based on the amino acid sequence of two peptides using the biased codon usage of *Acanthamoeba* (Hammer et al., 1987). Oligonucleotide A (5′-GGGGGCCGAGTCGGGGGCCCAGAGGATGA-AGGTGAT-3′) is complementary to nucleotides 238–273 (amino acid residues 80–91). Oligonucleotide B (5′-GC-CGTCCACCTGGAACTCGTAGTCGAAGATGGCGTA-3′) is complementary to nucleotides 187–222 (amino acid residues 63–74). These oligonucleotide probes were radiolabeled at their 5′ ends with [γ-^{32}P]ATP using T4 polynucleotide kinase and used to select a clone (λ2.1.1) with a 900 bp insert. The insert was released with *Eco*RI, isolated from an agarose gel using the Glassmilk method (Bio101, La Jolla, Ca), and subcloned into pUC18. The resulting construct, pSM1, was utilized for sequence analysis.

Nucleotide Sequence Determination. Double-stranded DNA sequencing was performed by the dideoxy termination method (Sanger et al., 1977) using Sequenase version 2.0 (USB). Sequencing was routinely carried out according to instructions provided by USB except that sequence labeling reactions were performed on ice. Both strands were fully sequenced using oligonucleotide primers constructed from sequence determined in the previous round of sequencing. Additional DNA sequencing was performed on λ2.1.1 using the Applied Biosystems Inc. Model 373A automatic DNA sequencer. Sequence analysis and database searches were performed using the GCG package of computer programs from the University of Wisconsin running on a VAX 8530 computer.

Construction of an Actophorin Expression Plasmid. The expression plasmid pACT was created using polymerase chain reaction (PCR) directed mutagenesis of λ2.1.1. A unique *Nde*I site was introduced prior to the initiation ATG codon using the oligonucleotide 5′-CGGAATTCATATGTCC-GGCATTGCTGTCTCTGACGA-3′. This changed the two underlined base pairs in the 5′-noncoding region of the sequence but not the amino acid sequence. Similarly, a unique *Bam*HI site was introduced at the 3′ end of the coding sequence immediately downstream from the TAG termination codon using the oligonucleotide 5′-AGAGGTGGGGACAGAGG-GATCCCGTCTA-3′. The final PCR product was digested with *Nde*I and *Bam*HI and ligated into the expression vector pMW172 (Rosenberg et al., 1987) which had been digested with *Nde*I and *Bam*HI and dephosphorylated. The sequence of the expression construct was verified by DNA sequencing.

Expression and Purification of Recombinant Actophorin. Plasmid pACT containing BL21(DE3) cells (Rosenberg et al., 1987) was grown at 37 °C in Luria broth supplemented with 60 μg/mL ampicilin from a 2% inoculum. IPTG was added to a final concentration of 1 mM when the cells had reached an A_{595} value of 1.0 (in approximately 3-h post-inoculation). Cell growth continued for 5 additional h before harvesting. Typically, 3 g of cells was obtained per liter.

Cells were pelleted by centrifugation at 10000*g* for 10 min and resuspended in 1 volume of 10 mM Tris-HCl, pH 8.0. The cells were respun as above and resuspended in 2 volumes of 10 mM Tris (pH 8.0)/1 mM EDTA/1 mM sodium azide (buffer I). The cells were disrupted by two passages through a French press. The extract was clarified by centrifugation at 12000*g* for 20 min, and the supernatant was designated as fraction I.

Fraction I was diluted to a final concentration of 10 mg/mL with buffer I. Then 400 mg of solid $(NH_4)_2SO_4$ was added slowly to each milliliter of solution at 4 °C with constant stirring. After 30 min on ice, the solution was centrifuged for 30 min at 12000*g*, and the supernatant was decanted. Recombinant actophorin was precipitated from the supernatant by the addition of 300 mg of solid $(NH_4)_2SO_4$ per original milliliter of solution. The pellet was resuspended in 3 mL of buffer I and dialyzed versus 2 L of buffer I at 4 °C overnight. The dialysate was designated as fraction II.

Fraction II was chromatographed on a column of Sephadex G-75 (1.8 cm^2 × 110 cm) in buffer I. The major peak containing actophorin activity was pooled and concentrated to a final volume of 2 mL by pressure filtration through a semipermeable membrane (Amicon YM-3). The concentrated material constituted fraction III.

Fraction III was applied to a Mono Q column (0.2 cm^2 × 6 cm) in buffer I and eluted with a linear KCl gradient (0–60 mM) using a Pharmacia FPLC system. Homogeneous actophorin eluted at approximately 45 mM KCl. The pooled peak, designated fraction IV, was used without further modification unless otherwise noted.

Viscometry Assay. The apparent low-shear viscometry assay was performed essentially as described by Maclean-Fletcher and Pollard (1980). Briefly, 10 μM monomeric actin is polymerized in a 100-μL capillary tube (Corning Glass, New York, NY) containing various amounts of recombinant or native actophorin in 50 mM KCl, 1 mM $MgSO_4$, 1 mM EGTA, and 10 mM Tris-HCl, pH 8.0. Once mixed, the tubes are incubated at room temperature (approximately 25 °C) for 1 h. A steel ball is dropped through the suspension, and the time required for the ball to traverse the length of the tube is measured and is here defined as apparent viscosity. A unit of actophorin is the amount of protein (in micrograms) required to reduce the apparent low-shear viscosity by 50%.

Actin Polymerization Assay. Actin was labeled with *N*-(1-pyrenyl)iodoacetamide (Molecular Probes Inc., Eugene, OR) as described by Pollard (1984). Additionally, the pyrenylactin was further purified by dialysis against 2 L of 2 mM Tris-HCl, pH 8.0, 0.2 mM ATP, 0.2 mM $CaCl_2$, 0.5 mM DTT, and 3 mM sodium azide at 4 °C overnight followed by gel exclusion chromatography through Sephacryl S-300. Spontaneous polymerization at 25 °C was initiated by mixing actin monomers (6% pyrene labeled), actophorin, and concentrated salts to give a final buffer composition of 50 mM KCl, 1 mM $MgSO_4$, 1 mM EGTA, 0.2 mM ATP, 0.2 mM $CaCl_2$, 0.5 mM DTT, and 10 mM Tris-HCl, pH 8.0. The increase in pyrenylactin fluorescence during polymerization was moni-

tored at an emission wavelength of 407 nm (emission slit width of 10 nm) postexcitation at 365 nm (excitation slit width of 3 nm) on a Perkin-Elmer 650-10S spectrometer.

Monoclonal Antibodies and Antibody Assays. Monoclonal antibodies against native actophorin were produced and characterized according to Kiehart et al. (1984). The mice were immunized with 100 μg of pure actophorin isolated from *Acanthamoeba*. Enzyme-linked immunoadsorbant assays (ELISAs) were performed by adsorbing 1 μg of antigen (either native or recombinant actophorin) to the surface of 96-well microtiter plates (Immulon 2; Dynatech Laboratories, Chantilly, VA). After the wells were blocked with phosphate-buffered saline (PBS) supplemented with 10% nonfat dry milk, monoclonal antibodies in blocking solution were added at various dilutions and allowed to react with the antigen at room temperature for 1 h. Following three washes in PBS, goat anti-mouse antibody conjugated with horseradish peroxidase was added at a 1:2000 dilution (in blocking buffer) and incubated for 1 h at room temperature. After washing as above, color development is achieved by adding 100 μL of a solution containing 50 mM sodium citrate, 50 mM citric acid, 1 mg/mL *o*-phenylenediamine, and 0.006% H_2O_2. After suitable color development (typically 5–10 min of incubation at room temperature), 50 μL of 2 M sulfuric acid was added to stop the reaction and stabilize the product. Absorbance was measured using an automatic ELISA plate reader (Bio-Tek Instruments, Inc.). Western blots (Towbin et al., 1979) were made according to Kaiser et al. (1989).

Crystallization and X-ray Diffraction of Recombinant Actophorin. Purified recombinant actophorin (fraction IV) was dialyzed versus 4 L of 50 mM sodium acetate (pH 5.5), 2 mM DTT, and 1 mM sodium azide at 4 °C for 12 h. The dialyzed material was pressure-filtered as above to a final concentration of 5 mg/mL. Crystals were obtained by vapor diffusion through hanging drops at room temperature using poly(ethylene glycol) 8000 (PEG 8000) as the precipitant. Alternatively, recombinant actophorin fraction IV was dialyzed versus 4 L of 100 mM HEPES (pH 7.5), 2 mM DTT, and 1 mM sodium azide at 4 °C for 12 h and concentrated as above. Large isomorphous crystals were obtained as above using a combination of PEG 8000 and 2-propanol as the precipitating agents. CuKα X-rays were generated with a Rigaku RU-200 rotating-anode generator operating at 40 kV and 140 mA equipped with a graphite monochromator. Complete datasets were measured on single crystals at room temperature by ω scans of 0.25°. Frames were recorded for 240 s each. Diffraction measurements were collected by a Siemens/Nicolet multiwire area detector mounted on a Huber four-circle goniostat and processed using XENGEN (Howard et al., 1987).

RESULTS

Protein Sequence Analysis. We obtained much of the primary structure of actophorin by Edman degradation of purified peptide fragments produced by trypsin, CNBr and BNPS-skatole cleavage (Figure 1). Edman degradation of the intact native actophorin gave no yield, so that NH_2-terminus is blocked. We did not determine the blocking group. The peptide fragments gave a contiguous sequence spanning amino acid residues 14–135 (Figure 1). CNBr and BNPS-skatole fragments allowed us to order the tryptic peptides. CNBr-9 allowed the ordering of peptides T15-T11-T19, and CNBr-6 was important in ordering peptides T6-T2 and the COOH-terminus. The sequences of fragments derived from cleavage with 2-[(2-nitrophenyl)sulfenyl]-3-methyl-3-bromoindolenine yielded the alignment T20-T6. The region 6-13

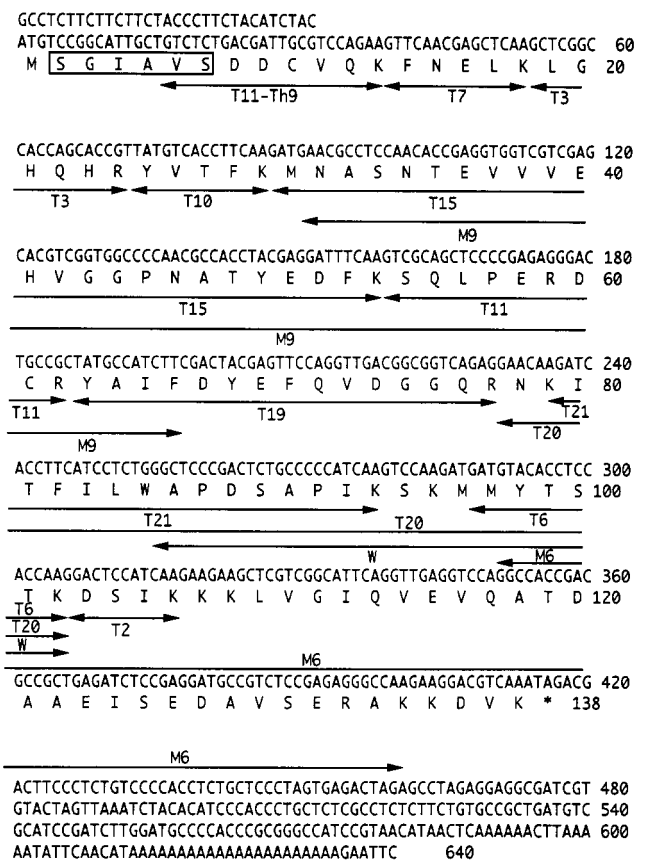

FIGURE 1: Nucleotide sequence of an *Acanthamoeba* actophorin cDNA and the deduced amino acid sequence of the coding region. Nucleotides and amino acids are numbered to the right of the sequence, starting from the A in the initiating codon for DNA and the initiating M for protein. The asterisk corresponds to the stop codon. The portion of the amino acid sequence confirmed by modified Edman degradation of purified recombinant actophorin is boxed. Arrowed lines beneath the amino acid sequence correspond to the ordered peptides generated by chemical or enzymatic cleavage of native actophorin. The designations employed are as follows: T, trypsin; M, cyanogen bromide; W, 2-[(2-nitrophenyl)sulfenyl]-3-methyl-3-bromoindolenine.

was contained in a thermolysin subfragment of the blocked tryptic peptide T11. This protein–chemical analysis covered the entire sequence except for the extreme NH_2-terminal and COOH-terminal residues of the protein. We looked for but did not observe modified amino acids in this analysis; furthermore, we could not assign cysteine residues.

Cloning and Sequencing of an Acanthamoeba Actophorin cDNA. The nucleotide sequence of a full-length actophorin cDNA clone contained a 414 bp open reading frame corresponding to a protein of 138 amino acid residues, with a calculated mass of 15 543 Da. The deduced amino acid sequence confirms the amino acid sequence determined by peptide analysis (Figure 1), provides the sequence of the extreme amino and carboxyl termini, and establishes the cysteine positions that were not available from the peptide analysis. There are no sequence ambiguities between the two methods. The cDNA is GC-rich and has the same highly restricted codon usage as other *Acanthamoeba* genes (Hammer et al., 1987). The cDNA sequence as illustrated in Figure 1 has been reported to Genbank and assigned Accession Number M93361.

The entire 5′-noncoding sequencing was refractory to complete sequence analysis, perhaps due to unusual secondary structure elements. The sequence of this region (approximately 300 bp) could not be determined either by automatic

Table I: Amino Acid Similarity/Identity for Actophorin versus Selected Actin Binding Proteins

actophorin versus	% similarity	% identity	sequence ref
human cofilin	66.2	41.2	Ogawa et al. (1990)
mosue cofilin	65.4	40.4	Moriyama et al. (1990a)
porcine cofilin	66.2	40.4	Matsuzaki et al. (1988)
chicken cofilin	62.5	38.2	Abe et al. (1990)
porcine destrin	61.0	36.8	Moriyama et al. (1990b)
chicken ADF	60.3	36.0	Adams et al. (1990)
echinoderm depactin	53.7	26.1	Takagi et al. (1988)

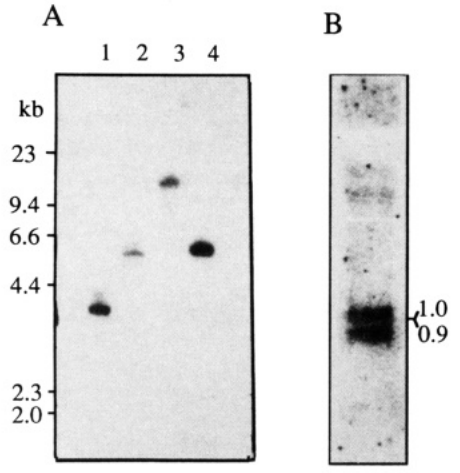

FIGURE 2: (A) Southern blot analysis of *Acanthamoeba* genomic DNA. Ten micrograms of genomic DNA is digested with *Hin*dIII (lane 1), *Eco*RI (lane 2), *Bgl*I (lane 3), or *Pst*I (lane 4) and electrophoresed on a 1% agarose gel. After Southern blotting, the nitrocellulose filter is probed with the entire ^{32}P-labeled actophorin cDNA and autoradiographed. (B) Northern blot hybridization analysis of total RNA isolated from *Acanthamoeba*. Twenty micrograms of total RNA is separated by electrophoresis in a 1.2% denaturing formaldehyde–agarose gel, transferred to a nitrocellulose membrane, and treated as in (A). The size of the transcripts is indicated.

sequencing or by sequencing with thermostable DNA polymerases at elevated temperature (data not shown). In addition, the 5′-noncoding region of the actophorin cDNA was unstable in plasmid constructs and was often found to be deleted. This was observed in several different plasmids and in several different genetic backgrounds (data not shown).

Sequence Similarity to Other Actin Binding/Severing Proteins. A FASTA search (Pearson & Lipman, 1988) of the Genbank Release 70 database revealed that actophorin has significant amino acid sequence similarities to cofilin, ADF, destrin, and depactin (Table I). Thirteen residues are identical in the eight proteins. The amino acid sequence of actophorin is closer to the cofilins than it is to destrin or ADF.

Actophorin Southern/Northern Analysis. Digests of *Acanthamoeba* genomic DNA with *Hin*dIII, *Eco*RI, *Bgl*I, or *Pst*I all yielded single bands that hybridize with the entire actophorin coding region (Figure 2A); hence, actophorin is a single-copy, intronless gene. Two distinct RNA species hybridize equally well with the actophorin cDNA (Figure 2B). The transcripts differ in size by about 100 bases The smaller message (0.9 kb) probably results in the cDNA of λ2.1.1 upon reverse transcription.

Overproduction and Isolation of Recombinant Actophorin. Bacteria with the expression plasmid pACT synthesize high levels of soluble and active actophorin (Figure 3, lane I). The solubility of the recombinant actophorin simplifies its purification. The falling-ball viscometry assay can measure the

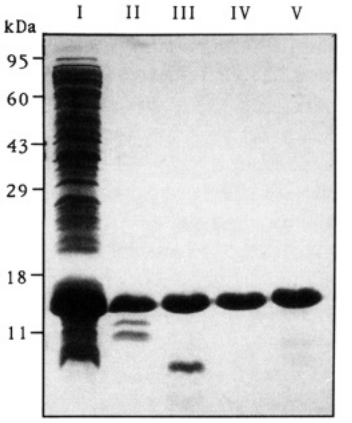

FIGURE 3: Purification of recombinant actophorin. Gel electrophoresis in 14% polyacrylamide with SDS of samples from each step in the purification of recombinant actophorin. Lane I, crude bacterial extract; lane II, $(NH_4)_2SO_4$ precipitate; lane III, Sephadex G-75 pool; lane IV, Mono Q pool. Lane V shows purified native actophorin for comparison. Protein loads are as follows: lane I, 20 μg; lane II, 15 μg; lanes III–V, 6 μg. Proteins are visualized by staining the gel with Coomassie brilliant blue. Molecular mass markers are indicated.

specific activity of actophorin in crude bacterial extracts due to the absence of eukaryotic actin binding proteins that normally mask or inhibit actophorin activity in *Acanthamoeba* preparations. Nearly homogeneous material results from the ammonium sulfate fractionation (Figure 3, lane II). The few remaining contaminating bands are removed by size-exclusion chromatography on Sephadex G-75 and by chromatography on Mono Q (Figure 3, lanes III and IV).

Overproduction of recombinant actophorin in induced BL21(DE3) cells harboring pACT, coupled with our modified purification procedure, yields 1.3 mg of pure recombinant actophorin per gram of bacterial cell paste in less than 1 week (Table II and Figure 3). This yield per gram of cells is 100 times higher than the purification from *Acanthamoeba* (Cooper et al., 1986). Edman degradation of the N-terminal region of purified recombinant actophorin (Figure 1) confirms the identity of the overexpressed material as bona fide actophorin and reveals that the initiating methionine residue is removed by *E. coli* as a posttranslational modification.

Physical Properties of Native and Recombinant Actophorin. The electrophoretic mobility of recombinant actophorin agrees with that predicted from the primary sequence and the native molecular weight established previously (Cooper et al., 1986). Recombinant actophorin is chromatographically and electrophoretically (Figure 3, lane V) indistinguishable from the native protein, including the observation that under nonreducing conditions the protein forms disulfide-linked dimers that elute from gel exclusion columns as a 30-kDa species (data not shown). By analytical gel filtration in Sephadex G75 (Siegel & Monty, 1966; data not shown), recombinant actophorin has a Stokes radius of 21 Å and a frictional ratio (f/f_0) of 1.3, values like the native protein (Cooper et al., 1986). Native isoelectric focusing experiments in polyacrylamide gels (data not shown) indicate that recombinant actophorin has a p*I* of 6.9 compared to a p*I* of 6.0 for native actophorin. This difference apparently arises from the lack of a blocked N-terminus in the recombinant protein.

The stabilities of native and recombinant actophorin assessed by urea denaturation profiles are identical (Figure 4). Both spectra show a decrease in the intrinsic tryptophan fluorescence with increasing urea concentrations. The midpoint of the single transition occurs between 3.0 and 3.5 M urea. Both proteins exhibit a 30-nm red shift in the maximal emission

Table II: Purification of Recombinant Actophorin

fraction	total units[a]	protein (mg/mL)	sp act. (units/mg)	recovery (%)	purification (*n*-fold)
(I) crude extract	250769	32.6	385	100	1
(II) ammonium sulfate	135000	1.5	5000	54	13
(III) Sephadex G-75	96000	1.5	8000	38	21
(IV) Mono Q	67826	1.3	8696	27	23

[a] The apparent low-shear viscometry assay was performed as described by Maclean-Fletcher and Pollard (1980). In order to quantitate the action of actophorin and as a purification aid, a unit of actophorin was defined and is the concentration of protein (in milligrams per milliliter) required to reduce the apparent viscosity by 50%.

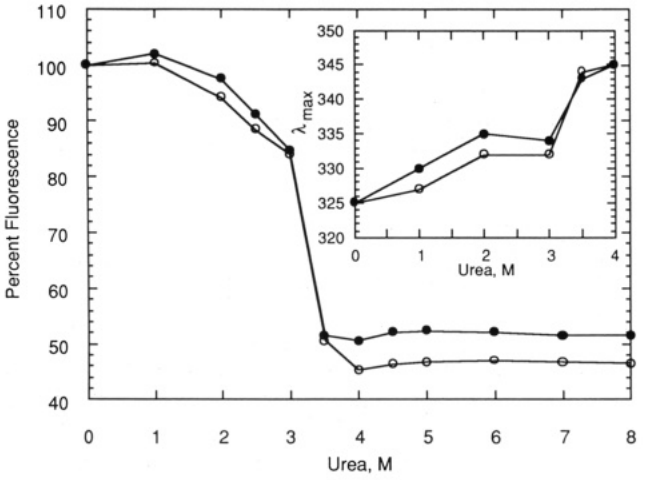

FIGURE 4: Urea denaturation profiles of native and recombinant actophorin. Tryptophan fluorescence intensity is measured as a function of urea concentration for 25 μM native (●) or recombinant (○) actophorin. Excitation at 295 nm (slit width 10 nm). Emission at 325 nm (slit width of 5 nm). Protein is diluted into the appropriate concentration of urea buffered with 20 mM Tris (pH 8.0). All measurements are made at room temperature. The inset illustrates the dependence of emission wavelength maximum on urea concentration.

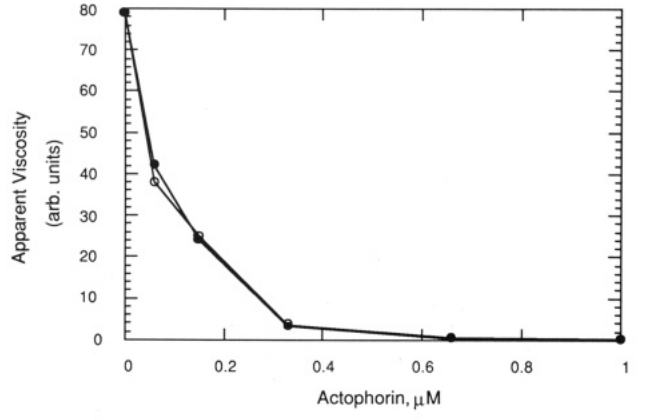

FIGURE 5: Reduction of low-shear viscosity by native and recombinant actophorin. 10 μM actin was polymerized for 1 h in 50 mM KCl, 1 mM $MgSO_4$, 1 mM EGTA, and 10 mM Tris-HCl, pH 8.0, with various amounts of native (●) or recombinant (○) actophorin.

wavelength at urea concentrations beyond the transition (Figure 4, inset). The emission wavelength maximum shifts from 325 nm (0.0 M urea) to 355 nm (8.0 M urea).

Functional Comparisons of Native and Recombinant Actophorin. Both the native and recombinant actophorins decrease the low-shear viscosity of actin filament gels to the same extent (Figure 5). This suggests that the N-terminal modification of the native protein, which is absent in the recombinant material, is not required for actophorin function. Substoichiometric concentrations of recombinant actophorin accelerated the spontaneous polymerization of pyrenylactin (Figure 6) like the native protein (Cooper et al., 1986; Maciver et al., 1991) in a dose-dependent manner.

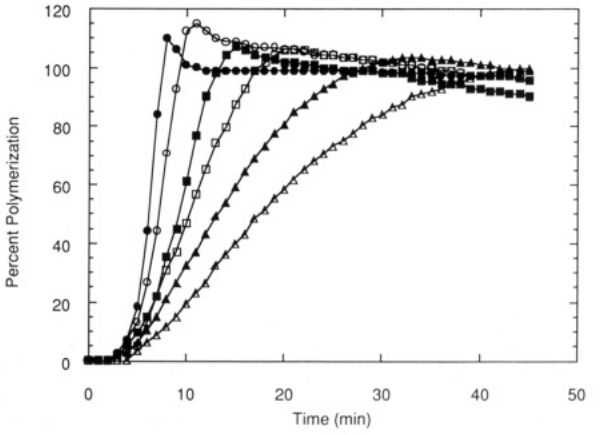

FIGURE 6: Spontaneous polymerization of pyrenylactin in the presence of recombinant actophorin. Polymerization of 2.5 μM pyrenylactin and various concentrations of recombinant actophorin: 2.5 (●), 1.2 (○), 0.9 (■), 0.6 (□), 0.3 (▲), and 0.0 μM (△). Relative pyrene fluorescence is converted to percent monomer polymerization by taking the value of the fluorescence plateau for the actin alone curve as 100% polymerization, and scaling all other curve points relative to that value.

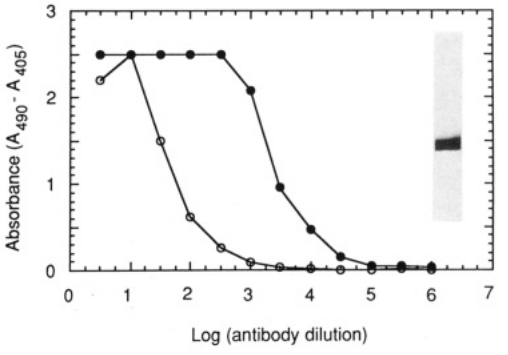

FIGURE 7: Comparison of the reactivity of native and recombinant actophorin with monoclonal antibody A1. Antibody binding is measured by solid-phase ELISA for native (●) or recombinant (○) actophorin immobilized on plastic wells. The concentration of the monoclonal antibody was 3.0 μg/mL. The ordinate is the absorbance measured at 490 nm minus the background at 405 nm. The insert is a Western blot of *Acanthamoeba* crude cell extracts probed with the monoclonal antibody.

Reactivity of Recombinant Actophorin with Monoclonal Antibodies. Recombinant and native actophorins differ in their reactivity for three different monoclonal antibodies raised to native actophorin (one example is shown in Figure 7). These monoclonal antibodies react with the recombinant protein, although compared with the native protein approximately 40-fold more antibody is required to saturate the assay. All three anti-actophorin monoclonal antibodies were specific for actophorin on Western blots of crude protein extracts of *Acanthamoeba* (one example is shown in Figure 7, insert.

Crystallization and X-ray Diffraction of Recombinant Actophorin. Diffraction-quality crystals of recombinant

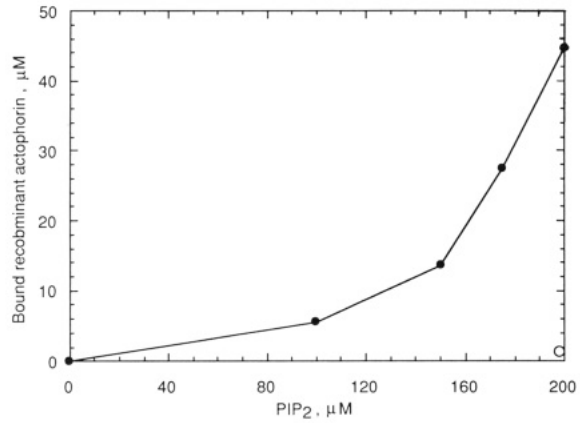

FIGURE 8: Binding of PIP_2 to recombinant actophorin. Recombinant actophorin at 60 μM was reacted with various amounts of phosphatidylinositol 4′,5′-bisphosphate, PIP_2 (Boehringer Mannheim), micelles in a buffer containing 10 mM Tris-HCl (pH 7.5)/75 mM KCl in a final reaction volume of 250 μL. Incubation was carried out at room temperature for 10 min, at which time the entire sample was loaded on a Sephadex G-100 column (43 cm × 0.2 cm^2) and chromatographed in the same buffer. Fractions (0.5 mL) were collected and analyzed for protein content. Bound protein was determined by subtracting the calculated amount of free protein (the area under the eluted actophorin peak) from 60 μM. The open circle shows that recombinant actophorin does not intract with 200 μM phosphatidylserine.

actophorin formed routinely in 3–5 days. Crystals are obtained using 18–20% (w/v) PEG 8000, a lower concentration than has been previously described (Magnus et al., 1988). Like the crystallization of the native protein, the inclusion of a reducing agent (DTT) is required for proper crystal formation. Crysals form as thick prismatic needles with approximate dimensions of 1.0 mm × 0.08 mm × 0.04 mm. Thicker prismatic needle crystals can be obtained by using 20% (w/v) PEG 8000/10% (v/v) 2-propanol buffered in 100 mM HEPES (pH 7.5) as precipitants. These crystals grow to approximate dimensions of 1.0 mm × 0.1 mm × 0.1 mm. The crystal habit of recombinant actophorin (obtained by both precipitation methods) is similar to that of native protein crystals. X-ray diffraction measurements confirm that the space group of the PEG 8000/2-propanol recombinant actophorin crystals is $P2_12_12_1$, the same as the native crystal space group. The area detector data collection statistics presented in Table III show that the recombinant crystal form is better suited for structure determination studies than the native crystal form. The lower R_{sym} and B values for the recombinant actophorin crystals indicate that these crystals have higher internal order than do the native crystals. This may be due to the absence of N-terminal modifications present in the native material. The recombinant actophorin crystals diffract more intensely than the native protein crystals as evidenced by the almost doubling of the $\langle I \rangle / \sigma$ value. Both the native and recombinant crystals diffract to approximately the same resolution, and the unit cell volumes differ by only 0.7%.

Binding of PIP_2 to Recombinant Actophorin. PIP_2 micelles interact with recombinant actophorin in a concentration-dependent fashion as assayed by small-zone gel filtration (Figure 8). This interaction is specific, as recombinant actophorin has no affinity for phosphatidylserine (Figure 8, open circle). Binding interactions are observed at PIP_2:actophorin ratios ranging from 1.7:1 to 3.3:1. At the lower ratio, only 9% of the protein is bound, while at the higher ratio 74% of the protein is bound. By fitting the binding curve to a second-order polynomial and extrapolating, it is possible to bind all of the recombinant actophorin at a PIP_2 concentration of 225 μM. This corresponds to 3.75 PIP_2 molecules bound per molecule of actophorin.

Table III: Crystal and X-ray Data Collection Statistics for Native and Recombinant Actophorin

parameter	actophorin	
	native	recombinant
space group	$P2_12_12_1$	$P2_12_12_1$
unit-cell parameters (Å)		
a	39.8	39.6
b	47.3	47.6
c	69.9	69.3
$\alpha = \beta = \gamma$ (deg)	90.0	90.0
diffraction data		
observations (no.)	14822	23041
unique reflections (no.)	3576	4446
completeness (%) to 2.6 Å	76.3	94.2
completeness (%) to 2.5 Å	71.8	86.2
$\langle I \rangle / \sigma$[a]	12.3	22.4
B (Å^2)[b]	36.2	31.5
R_{sym}[c]	0.093	0.051

[a] $\langle I \rangle / \sigma$ is the average intensity divided by the standard deviation for all reflections. [b] B is the overall Debye–Waller temperature factor. [c] $R_{sym} = \sum_h \sum_i |I(h)_i - \langle I(h) \rangle| / \sum_h \sum_i I(h)_i$, where $I(h)$ is the intensity of reflection h, $\sum_h$ is the sum over all reflections, and $\sum_i$ is the sum over the ith measurement.

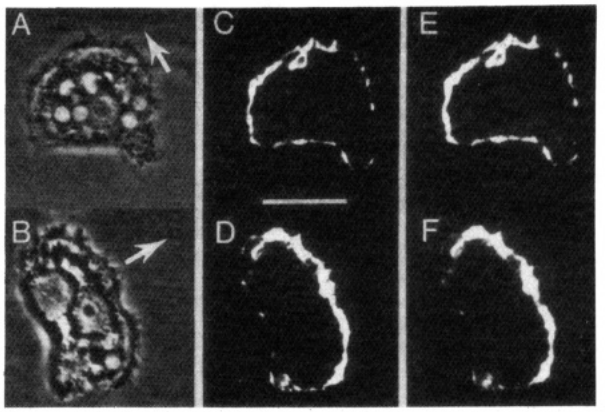

FIGURE 9: Confocal fluorescence and phase-contrast micrographs of *Acanthamoeba* stained with rhodamine–phalloidin and two different monoclonal antibodies to actophorin. Samples were prepared for immunofluorescence microscopy by the method of Yonemura and Pollard (1992), except that samples were mounted on glass slides in Vectashield (Vector Laboratories, Burlingame, CA) prior to microscopy. Scanning laser confocal microscopy was performed using a BioRad MRC-600 microscope, and images were photographed from a high-resolution monitor. (A, B) Phase-contrast images of locomoting cells fixed with a mixture of methanol and formaldehyde. Arrows indicate the direction of locomotion. (C, D) Laser scanning confocal fluorescence micrograph of cells from (A) and (B) stained with anti-actophorin monoclonal antibodies: A.1 (C) and A.2 (D). (E, F) Laser scanning confocal fluorescence micrograph of cells from (A) and (B) stained with rhodamine–phalloidin to indicate actin filaments. Bar, 15 μm.

Fluorescent Antibody Localization of Actophorin. Actophorin is concentrated in the cortex of *Acanthamoeba* (Figure 9C,D) together with rhodamine–phalloidin-stained actin filaments (Figure 9E,F). The staining for both actophorin and actin filaments was most prominent at the part of the cell that appears by morphological criteria to be the leading edge during movement. In about 20% of cells, the edge of a large internal vacuole is brightly stained with both anti-actophorin (Figure 10A) and rhodamine–phalloidin. Another 10% of stained cells have an irregular cup-shaped surface appendage (Diaz et al., 1991) that stained for both actophorin and actin filaments (Figure 10B,C). There was no detectable nuclear staining. Two different fixation techniques [1% formaldehyde

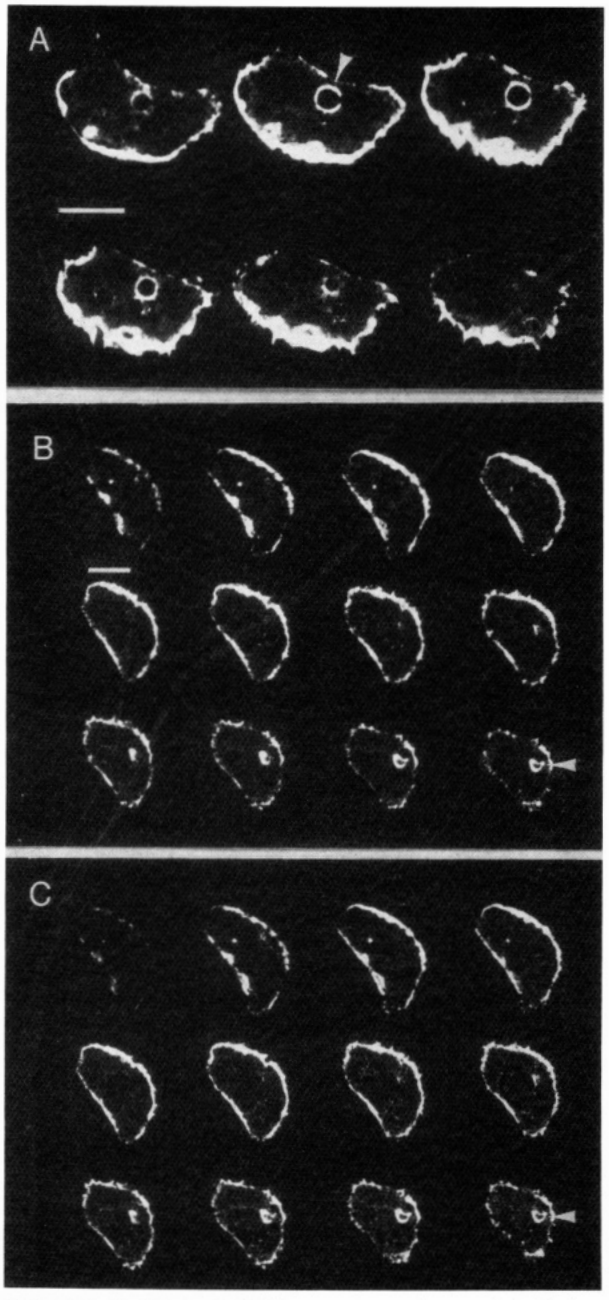

FIGURE 10: Serial confocal fluorescence micrographs of *Acanthamoeba* stained with anti-actophorin monoclonal antibody A.1 (A and B) and rhodamine–phalloidin (C). Methods are as in Figure 9. (A) Optical sections of locomoting cell. Arrowhead indicates the contractile vacuole. Upper left, basal surface of cell; lower right, top surface. Bar, 10 μm. (B, C) Optical sections of a locomoting cell. Arrowheads indicate an amoebastome. Upper left, basal surface of cell; lower right, top surface. (B) Antiactophorin monoclonal antibody staining. (C) Rhodamine–phalloidin staining. Bar, 10 μm.

in methanol or 100% methanol (Yonemura & Pollard, 1992)], three different monoclonal antibodies (A.1, A.2, and A.3), and all combinations of staining and fixation gave indistinguishable results. Second antibody alone did not stain the cells (data not shown). Additionally, all the labeling studies above were performed as single-label experiments (data not shown) to control for possible artifacts or fluorescence signal bleeding between the rhodamine and fluorescein channels. The fluorescent antibody staining was identical in the single- and double-label experiments.

DISCUSSION

The primary structure confirms that *Acanthamoeba* actophorin is a member of the family of small monomer binding/filament severing proteins isolated from diverse species. Actophorin is over 60% similar to the cofilins and actin depolymerizing protein (e.g., porcine destrin) from vertebrates (Table I and Figure 2), including 13 amino acid residues that are positionally conserved in the entire family. The similarity is particularly striking around two sites implicated in the binding of cofilin to actin. The first is the DAIKKK amino acid sequence of cofilin (amino acid residues 123–128). This peptide competes with cofilin for binding to actin monomers (Matsuzaki et al., 1988) and is contained in actophorin as the sequence DSIKKK (residues 103–109). The second conserved sequence is in the region of the cofilin dodecapeptide WAPESAPLKSKM (residues 104–115). This sequence has been shown to be a site of actin monomer binding (Yonezawa et al., 1991) and corresponds to the actophorin peptide WAPDSAPIKSKM (residues 85–96). Point mutations of Lys114 reduce the affinity of cofilin for F-actin with a parallel decrease in filament severing (Moriyama et al., 1992). Substitutions of both Lys112 and Lys114 resulted in a complete lack of F-actin binding. The sequence of actophorin is closer to the amino acid sequence of cofilin than it is to the sequence of destrin or ADF. This is surprising considering that biochemical properites of actophorin are more similar to destrin/ADF. In particular, cofilin binds to actin filaments (Yonezawa et al., 1985; Nishida, 1985) while actophorin severs actin filaments but does not bind tightly to them. Atomic structures of these proteins will be required to understand the basis of these differences.

The major difference between actophorin and all of the related proteins is that actophorin is shorter by approximately 30 residues. In general, there are five small internal regions in cofilin not represented in actophorin. One of the deletions removes an SV40 large T-antigen-type nuclear transport signal, PXXXKKRKAV (Kalderon et al., 1984). It is not known whether the nuclear targeting of the actin-modulating proteins is important to cytoskeletal actin regulation in higher organisms or serves some other unrelated function. Accordingly, no actophorin was detected in the nucleus by fluorescent antibody staining.

In contrast, despite sequence similarities, neither the monoclonal antibodies used in this study nor polyclonal antibodies cross-react with protein extracts of other species, including yeast (data not shown). Additionally, there is no cross-reactivity of polyclonal antibodies between actophorin and depactin (T. D. Pollard and I. Mabuchi, unpublished observations). Bamburg and Bray (1987) also found that antibodies against chicken embryonic brain ADF do not recognize *Acanthamoeba* proteins. Clearly, the 35 amino acids shared by destrin and actophorin are insufficient for antibody cross-reactivity.

The purification procedure outlined in Table II yields a large amount of homogeneous actophorin that is indistinguishable from the native protein in most ways. The identical stability in urea and the formation of crystals of the same space group with nearly identical unit-cell dimensions indicate very similar three-dimensional structures. The decrease in quantum yield upon denaturation in urea may indicate that the single tryptophan of actophorin is relatively isolated from side chain interactions in the folded molecule. Additionally, recombinant actophorin accelerates the rate of spontaneous pyrenylactin polymerization by severing actin filaments in a dose-dependent fashion. The kinetics of actin filament severing by recombinant actophorin observed by the pyrenylactin polymerization assay are in accord with similar experiments with the native material (Maciver et al., 1991). Like native

actophorin (Maciver et al., 1991), recombinant actophorin has no effect on the lag period of the pyrenylactin polymerization process, or any significant effect on the steady-state concentration of actin filaments.

Remarkably, although recombinant actophorin has chromatographic, hydrodynamic, and stability properties similar to native actophorin, it reacts weakly with three different monoclonal antibodies by ELISA. The epitopes for these monoclonals have not been mapped, but a possible explanation is that the posttranslational modifications of the NH_2-terminus of the native protein, the only known modification of the native protein, might constitute part of a major epitope. The charge difference might also influence the adsorption of the proteins to the ELISA wells.

Recombinant actophorin interacts with PIP_2, like related proteins [e.g., see Yonezawa et al. (1990)]. Yet the physiological implications of polyphosphoinositide binding are not clear. The interaction, however, does seem to be specific, as actophorin does not bind to phosphatidylserine in small-zone gel filtration assays. Studies to carefully determine kinetic binding constants between actophorin (or any other member of the actophorin-like family) and polyphosphoinositides are needed.

The colocalization of actophorin and actin in the cortex of *Acanthamoeba* may provide some clues about the functions of actophorin. Given the low affinity of actophorin for actin filaments, we did not anticipate that they would be found together in the cytoplasm. Perhaps the concentration of actin in the cortex (on the order of 1 mM) is high enough to drive the binding of actophorin simply by mass action. If so, the actophorin may play an active role in limiting the length of the cortical actin filaments and promoting the assembly of actin filament bundles as demonstrated *in vitro* (Maciver et al., 1991b). Severing of actin filaments without capping may also contribute to the rapid assembly and turnover of actin filaments observed in the cortex of other cells especially at the leading edge of locomoting cells [e.g., see Wang (1985) and Forscher and Smith (1988)]. For example, if actophorin severed filaments once they reached some critical size, this would expose a new barbed end with ADP–actin which would tend to depolymerize.

The existence of two actophorin transcripts may represent alternative splicing products or the processing of larger transcripts. Since we have no evidence for actophorin isomers from gel electrophoresis, isoelectric focusing, or protein sequencing, the two transcripts most probably code for the same protein. In contrast, *Acanthamoeba* express at least three isoforms of profilin (Pollard & Rimm, 1991).

The cloning of the gene encoding actophorin, and the expression and purification of large amounts of the recombinant protein, is an important step in our effort to determine its structure. The recombinant protein not only forms superior crystals but also has been modified with selenomethionine for phase determination. The three-dimensional structure of *Acanthamoeba* actophorin should shed light on the mechanism of action of the entire family of small actin monomer binding/actin filament severing proteins.

ACKNOWLEDGMENT

We thank Dr. Ludwig Brand for discussion of the urea denaturation experiments, Dr. David Rimm for aid with the cloning, and Dr. Laura Machesky for advice on lipid binding assays. Dr. Eaton E. Lattman is especially thanked for his critical reading of the manuscript and for his helpful discussions of the experimental results.

REFERENCES

Abe, H., Endo, T., Yamamoto, K., & Obinata, T. (1990) *Biochemistry 29*, 7420–7425.

Adams, M. E., Minamide, L. S., Duester, G., & Bamburg, J. R. (1990) *Biochemistry 29*, 7414–7420.

Ampe, C., Sato, M., Pollard, T. D., & Vandekerckhove, J. S. (1988) *Eur. J. Biochem. 170*, 597–601.

Bamburg, J. R., & Bray, D. (1987) *J. Cell Biol. 105*, 2817–2825.

Bamburg, J. R., Harris, H. E., & Weeds, A. G. (1980) *FEBS Lett. 121*, 178–182.

Bradford, M. M. (1976) *Anal. Biochem. 72*, 248–254.

Cooper, J. A., Blum, J. D., Williams, R. C., & Pollard, T. D. (1986) *J. Biol. Chem. 261*, 477–485.

Davison, M. W., & Critchley (1988) *Cell 52*, 159–160.

Diaz, J., Osuna, A., Rosales, M. J., Cifuentes, J., & Mascaro, C. (1991) *Int. J. Parasitol. 21*, 365–367.

Forscher, P., & Smith, S. J. (1988) *J. Cell Biol. 107*, 1505–1516.

Hammer, J. A., Bowers, B., Paterson, B. M., & Korn, E. D. (1987) *J. Cell Biol. 105*, 913–925.

Howard, A. J., Gilliland, G. L., Finzel, B. C., & Poulos, T. L. (1987) *J. Appl. Crystallogr. 20*, 383–387.

Kaiser, D. A., Goldschmidt-Clermont, P. J., Levine, B., & Pollard, T. D. (1989) *Cell Motil. Cytoskeleton 14*, 251–262.

Kalderon, D., Roberts, B. L., Richardson, W. D., & Smith, A. E. (1984) *Cell 39*, 499–509.

Kiehart, D. P., Kaiser, D. A., & Pollard, T. D. (1984) *J. Cell Biol. 99*, 1002–1014.

Koenig, M., Monaco, A. P., & Kunkel, L. M. (1988) *Cell 53*, 219–228.

Koffer, A., Edgar, A. J., & Bamburg, J. R. (1988) *J. Muscle Res. Cell Motil. 9*, 320–328.

Mabuchi, I. (1981) *J. Biochem. 89*, 1341–1344.

Maciver, S. K., Zot, H. G., & Pollard, T. D. (1991a) *J. Cell Biol. 115*, 1611–1620.

Maciver, S. K., Wachsstock, D. H., Schwarz, W. H., & Pollard, T. D. (1991b) *J. Cell Biol. 115*, 1621–1628.

MacLean-Fletcher, S. D., & Pollard, T. D. (1980) *J. Cell Biol. 85*, 414–428.

Magnus, K. A., Maciver, S. K., & Pollard, T. D. (1988) *J. Biol. Chem. 263*, 18143–18144.

Maniatis, T., Fritch, E. F., & Sambrook, J. (1981) *Molecular Cloning: A Laboratory Manual*, Cold Spring Harbor Laboratory, Cold Spring Harbor, NY.

Matsuzaki, F., Matsumoto, S., Yahara, I., Yonezawa, N., Nishida, E., & Sakai, H. (1988) *J. Biol. Chem. 263*, 11564–11568.

Moriyama, K., Matsumoto, S., Nishida, E., Sakai, H., & Yahara, I. (1990a) *Nucleic Acids Res. 18*, 3053.

Moriyama, K., Nishida, E., Yonezawa, N., Sakai, H., Matsumoto, S., Iida, K., & Yahara, I. (1990b) *J. Biol. Chem. 265*, 5678–5773.

Moriyama, K., Yonezawa, N., Sakai, H., Yahara, I., & Nishida, E. (1992) *J. Biol. Chem. 267*, 7240–7244.

Nishida, E. (1985) *Biochemistry 24*, 1160–1164.

Nishida, E., Maekawa, S., & Sakai, H. (1984) *Biochemistry 23*, 5307–5313.

Nishida, E., Muneyuki, E., Maekawa, S., Ohta, Y., & Sakai, H. (1985) *Biochemistry 24*, 6624–6630.

Ogawa, K., Tashima, M., Yumoto, Y., Okuda, T., Sawada, H., Okuma, M., & Maruyama, Y. (1990) *Nucleic Acids Res. 18*, 7169–7179.

Ohta, Y., Endo, S., Nishida, E., Murofushi, H., & Sakai, H. (1984) *J. Biochem. 96*, 1547–1558.

Pearson, W. R., & Lipman, D. J. (1988) *Proc. Natl. Acad. Sci. U.S.A. 85*, 2444–2448.

Pollard, T. D. (1984) *J. Cell Biol. 99*, 769–777.
Pollard, T. D., & Rimm, D. L. (1991) *Cell Motil. Cytoskeleton 20*, 169–177.
Rosenberg, A. H., Lade, B., Chui, D., Lin, S., Dunn, J., & Studier, F. W. (1987) *Gene (Amsterdam) 56*, 125–135.
Sambrook, J., Fritch, E. F., & Maniatis, T. (1989) *Molecular Cloning: A Laboratory Manual*, 2nd ed., Cold Spring Harbor Laboratory, Cold Spring Harbor, NY.
Sanger, F., Nicklen, S., & Coulson, A. R. (1977) *Proc. Natl. Acad. Sci. U.S.A. 74*, 5643–5647.
Siegel, L. M., & Monty, K. J. (1966) *Biochim. Biophys. Acta 112*, 346–362.
Sinard, J. H., & Pollard, T. D. (1989) *Cell Motil. Cytoskel. 12*, 42–52.
Takagi, T., Konishi, K., & Mabuchi, I. (1988) *J. Biol. Chem. 263*, 3097–3102.
Towbin, H., Staehelin, T., & Gordon, J. (1979) *Proc. Natl. Acad. Sci. U.S.A. 87*, 2740–2744.
Wang, Y. L. (1985) *J. Cell Biol. 101*, 597–602.
Yonemura, S., & Pollard, T. D. (1992) *J. Cell Sci. 102*, 629–642.
Yonezawa, N., Nishida, E., & Sakai, H. (1985) *J. Biol. Chem. 260*, 14410–14412.
Yonezawa, N., Nishida, E., Iida, K., Yahara, I., & Sakai, H. (1990) *J. Biol. Chem. 265*, 8382–8386.